

Liquid-Metal Microdroplets Formed Dynamically with Electrical Control of Size and Rate

Shi-Yang Tang, Ishan D. Joshipura, Yiliang Lin, Kourosch Kalantar-Zadeh, Arnan Mitchell, Khashayar Khoshmanesh,* and Michael D. Dickey*

Gallium based eutectic alloys such as EGaln (75% gallium, 25% indium) and Galinstan (68.5% gallium, 21.5% indium, 10% tin) are liquid metals with many useful properties, including high electrical and thermal conductivity, large surface tension, negligible vapor pressure, and low viscosity.^[1,2] Perhaps most importantly, these alloys provide an alternative to mercury, which is toxic. These extraordinary properties are useful for developing novel reconfigurable/stretchable electronics,^[3–6] interconnects,^[7] soft sensors,^[8,9] microfluidics actuators,^[10,11] and chemical sensors.^[12,13]

In particular, microdroplets of liquid metal can be used either as the core or as building blocks of systems that utilize the metal such as microswitches,^[14] pumps,^[11] mixers,^[10] motors,^[15] electrochemical sensors,^[12] 3D microelectrodes and microfins,^[16] 3D printed structures,^[17] conductive composites,^[18] inks for inkjet printing,^[19] and energy harvesting devices.^[20] In addition, liquid metal microdroplets with uniform size can assemble into periodic structures that may make them suitable for applications in optics such as radio frequency resonators^[21] and reconfigurable optical diffraction gratings.^[22,23]

Methods such as sonication,^[12,15,24] molding,^[25] and flow-focusing^[26–28] can produce liquid metal microdroplets. Sonication of liquid metal in a nonsolvent is a simple approach for producing micro to nanosized droplets. However, sonication produces polydisperse microdroplets, with the diameter ranging from a few hundred nano to several micrometers.^[12,15,24] Liquid metal spheres can be made by spreading liquid metal onto a topographical mold patterned with cylindrical reservoirs.^[25] Despite its simplicity, the smallest metal spheres produced using this method have diameters limited to $\approx 100 \mu\text{m}$, and producing a large number of such microdroplets using this method could be time consuming.

Microfluidic flow-focusing devices have been used widely to produce monodisperse microdroplets for chemical, biochemical and materials science applications.^[29] Such devices have

also been used to continuously produce monodisperse liquid metal microdroplets.^[26–28] Typically, flow-focusing devices force two immiscible fluids through a small orifice in a microfluidic device. Under the right set of conditions, flow through the orifice causes one stream of fluid to pinch off into discrete droplets within a continuous stream of the other fluid. Interfacial tension, inertia, and shear are important factors that dictate the size of droplets produced by flow-focusing. Increasing the shear rate decreases the size of the microdroplets produced by this technique. Due to their high surface tension, liquid metals only pinch off into microdroplets when the continuous phase generates sufficient shear.^[26,27] Thus, it is only possible to tune the diameter of droplets over a finite range by varying the shear rate, which depends on the viscosity of the continuous phase and the flow rates through the orifice. However, producing droplets smaller than the width of the orifice has yet to be reported because it requires prohibitively large pressures to achieve the necessary shear rates.^[26–28] These large pressures can physically compromise the microchannels or cause fluids to leak. More importantly, it is not straightforward to change the experimental conditions necessary to tune the size of the microdroplets produced by flow-focusing. Changing the viscosity of the continuous phase requires changing temperature or switching fluids, neither of which can be done quickly. Changing the flow rates can be done easily, but results in relatively long transition times (i.e., on the order of 10 s) for the flows to reach stable conditions, during which time many particles form without control of diameter.

In this work, we introduce a novel yet simple approach to rapidly vary and tune the size of liquid metal microdroplets by controlling the interfacial tension of the metal using both electrochemistry and electrocapillarity by applying an electrical potential to the liquid metal stream. The use of electrical potential is easy to implement and miniaturize, and controls the droplet size without altering any other experimental variables. Proof-of-concept experiments show the capability of using voltage to control and vary nearly instantly (i.e., within microseconds) the size of the liquid metal microdroplets produced by flow-focusing.

Figure 1A shows the schematic of the microfluidic flow-focusing device composed of molded poly(dimethylsiloxane) (PDMS) bonded onto a glass slide after oxygen plasma treatment. The chip has two inlets. A solution of glycerol–NaOH enters one inlet as the continuous phase and EGaln enters the other inlet as the discrete phase. The solution of glycerol–NaOH consists of 10 M NaOH aqueous solution mixed with glycerol at a ratio of 1:9 (v/v). We optimized empirically the ratio of glycerol to NaOH to achieve several goals. The glycerol increases the viscosity of the solution, which is necessary to create small

Dr. S.-Y. Tang, Prof. K. Kalantar-Zadeh, Prof. A. Mitchell,
Dr. K. Khoshmanesh
School of Electrical and Computer Engineering
RMIT University
Melbourne, VIC 3001, Australia
E-mail: khashayar.khoshmanesh@rmit.edu.au
I. D. Joshipura, Y. Lin, Prof. M. D. Dickey
Department of Chemical and Biomolecular Engineering
North Carolina State University
Raleigh, NC 27695, USA
E-mail: mddickey@ncsu.edu



DOI: 10.1002/adma.201503875

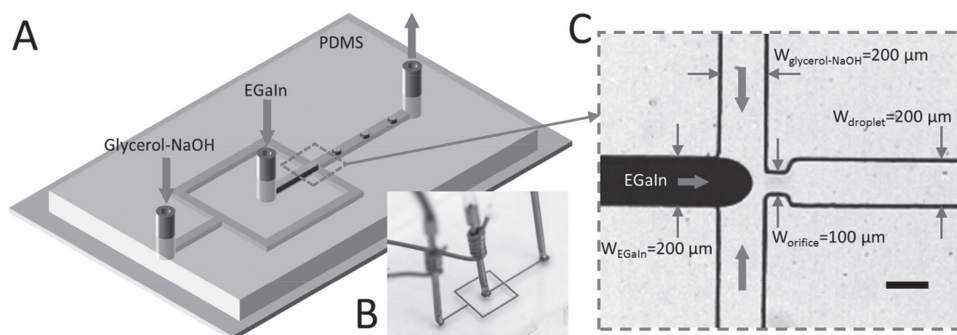


Figure 1. Experimental setup. A) A schematic of the experimental setup for forming liquid metal microdroplets. B) Photograph of the setup. C) Microscopy image of the flow-focusing section of the microfluidic chip. Scale bar is 200 μm .

droplets of EGaIn. NaOH removes the oxide layer that forms on EGaIn and therefore keeps the EGaIn surface pristine in the absence of oxidative potentials. It also provides ions for conducting current in glycerol. Stainless steel tubes wrapped with copper wires provide electrical contacts at the inlets, as shown in Figure 1B. Figure 1C shows a microscopy image of the system. The microchannels have a width and height of 200 and 75 μm , respectively, while the orifice has a width of 100 μm .

The diameter of microdroplets produced by flow-focusing varies inversely with the capillary number.^[30] The capillary number is a ratio of viscous forces to interfacial forces and in such a flow-focusing device is calculated using the following equation:^[30]

$$Ca_{\text{EGaIn}} = \frac{W_{\text{EGaIn}} \mu Q}{2h W_{\text{glycerol-NaOH}} \gamma} \left(\frac{1}{W_{\text{orifice}}} - \frac{1}{2W_{\text{EGaIn}}} \right) \quad (1)$$

where μ and Q are the viscosity and flow rate of the glycerol-NaOH solution, respectively, γ is the interfacial tension between EGaIn and the glycerol-NaOH solution, h is the height of the microchannel, while W_{orifice} , W_{EGaIn} , and $W_{\text{glycerol-NaOH}}$ are the widths of the orifice, liquid metal inlet, and glycerol-NaOH solution inlet, respectively, as presented in Figure 1C. In our design, $W_{\text{EGaIn}} = W_{\text{glycerol-NaOH}} = 2W_{\text{orifice}}$, and thus Equation (1) can be simplified as:

$$Ca_{\text{EGaIn}} = \frac{3\mu Q}{4h W_{\text{glycerol-NaOH}} \gamma} \quad (2)$$

Goniometer measurements estimate γ as $451 \pm 15 \text{ mN m}^{-1}$ (Supporting Information, Section S1). There are two ways to lower the interfacial tension. The application of a positive (oxidative) bias to the metal drives the formation of a surface oxide that acts as a surfactant and lowers the interfacial tension of EGaIn.^[31] Likewise, the application of a negative (reducing) bias places charge at the metal-solution interface that lowers interfacial tension via electrocapillarity.^[31] Lowering the interfacial tension increases the Capillary number according to Equation (2), and thus leads to the generation of smaller microdroplets of EGaIn. According to this hypothesis, the largest droplets should form in the absence of potential.

To test this hypothesis, we connected the liquid metal inlet tube to the anode while connecting the inlet tube for the glycerol-NaOH solution to the cathode. EGaIn and glycerol-NaOH flowed into the chip at rates of 5 and 50 $\mu\text{L min}^{-1}$, respectively, to generate EGaIn liquid metal droplets. **Figure 2A** presents

the uniform EGaIn microdroplets produced in the absence and presence of DC voltage (Movie S1, Supporting Information). In the absence of DC voltage, the EGaIn microdroplets have a diameter of $\approx 200 \mu\text{m}$. Interestingly, in the presence of DC voltage, the diameter of EGaIn microdroplets decreases to $\approx 150 \mu\text{m}$ in response to 2 V, and decreases further to $\approx 100 \mu\text{m}$ (equal to W_{orifice}) in response to 18 V (limit of our DC signal source), which is half the size of those produced at 0 V. Since the flow rate of liquid metal remains constant, the decrease in microdroplet diameter correlates with an increased number of droplets produced per second (Figure 2A). (Note: Although the flow rate of the syringe pump remains constant in these experiments, there is some minor variation in flow rate, perhaps due to bulging of the syringes and tubing at these high pressures.) Moreover, application of a large positive DC voltage causes the liquid metal to pinch off closer to the orifice, leading to a more distorted meniscus after forming each droplet (Figure 2A).

Figure 2B,C present the sequential snapshots of the production of one EGaIn droplet in response to 0 and 18 V, respectively. Applying a DC voltage leads to the formation of a tip on the EGaIn meniscus (indicated by an arrow) once the microdroplet leaves the orifice (Figure 2C), which does not occur in the absence of DC voltage (Figure 2B). This tip is also shown clearly in Movie S1 (Supporting Information). The formation of such a tip indicates the presence of an oxide layer on the surface of the EGaIn meniscus. In 1 M NaOH, 1 V is sufficient to drive the electrochemical oxidation of EGaIn. However, 1 V is insufficient here since there is a potential drop from the anode to the surface of the metal due to resistance arising from the narrow geometry of the channels and the low conductivity of the continuous phase. To confirm the existence of such an oxide layer, we measured the electrical current passing through the interface, and conducted off-chip experiments under similar current densities to examine the formation of the oxide layer, as shown in Section S2 of the Supporting Information. The formation of the oxide layer significantly lowers the interfacial tension between EGaIn and the glycerol-NaOH solution, which makes it possible to produce smaller EGaIn microdroplets without increasing the flow rate of the continuous phase liquid.

Applying a negative DC voltage of -2 V can also decrease the size of the microdroplets, as shown in Figure 2D (Movie S2, Supporting Information). The minimum droplet diameter obtained is $\approx 134 \mu\text{m}$ in response to -5 V , and does not change significantly by further lowering the voltage down to -18 V . The

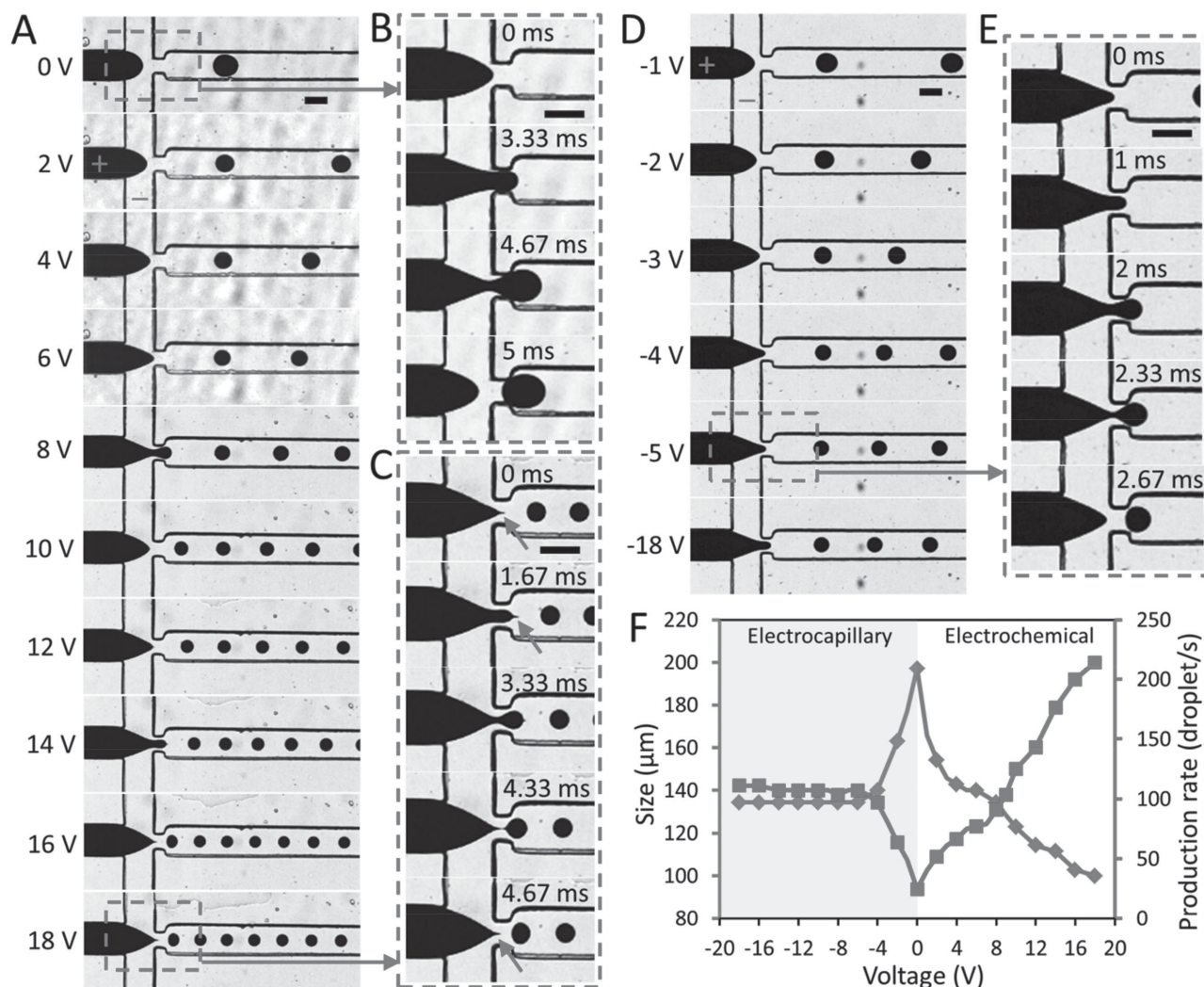


Figure 2. Electrochemical and electrocapillary control of the size of EGaIn microdroplets. A) Production of EGaIn microdroplets at positive voltages of 0–18 V. Sequential snapshots for producing one EGaIn microdroplet at voltages of B) 0 V and C) 18 V. D) Production of EGaIn microdroplets at negative voltages of –1 to –18 V. E) Sequential snapshots for producing one EGaIn microdroplet at a voltage of –5 V. F) Plot of size (squares) and production rate (diamonds) versus voltage. Scale bars are 200 μm.

application of a negative DC voltage lowers the surface tension of liquid metal via electrocapillarity. The negative voltage can also remove the oxide that may be present on the EGaIn meniscus via electrochemical reduction.^[31] The sequential snapshots given in Figure 2E show that a tip does not form on the EGaIn meniscus once the microdroplet leaves the orifice, confirming that the decrease of interfacial tension is not due to the formation of surface oxides. The decreased interfacial tension between EGaIn and glycerol–NaOH solution may be attributed to the change of voltage drop across the interface, as described by Lippmann's equation:^[32]

$$\gamma = \gamma_0 - \frac{1}{2} C_{\text{EDL}} V_{\text{EDL}}^2 \quad (3)$$

where γ_0 is the maximum interfacial tension when the voltage drop across the electrical double layer (EDL) at the interface is zero ($V_{\text{EDL}} = 0$), and C_{EDL} is the capacitance of the EDL. Applying a voltage increases the value of V_{EDL} , and therefore reduces the

interfacial tension, enabling the formation of smaller EGaIn microdroplets. The plateau in the drop size between –5 and –18 V suggests that V_{EDL} also plateaus, which is expected since Faradaic electrochemical reactions can occur with the continuous phase beyond a sufficiently large voltage (see Supporting Information, Section S2). It is likely that electrocapillary effects also occur at positive potentials, but previous studies suggest the presence of surface oxides at positive potentials dominates the interfacial behavior relative to electrocapillarity.^[31]

Figure 2F summarizes the variations of the size and number of EGaIn microdroplets with respect to the applied voltage. The device produces ≈ 25 droplets per second in the absence of a DC voltage. Applying 18 V to the metal increased the production rate to ≈ 215 droplets per second. Thus, the application of a modest voltage can change the frequency of droplet formation by an order of magnitude.

According to Equation (2), increasing the flow rate of the continuous phase liquid can also decrease the size of EGaIn

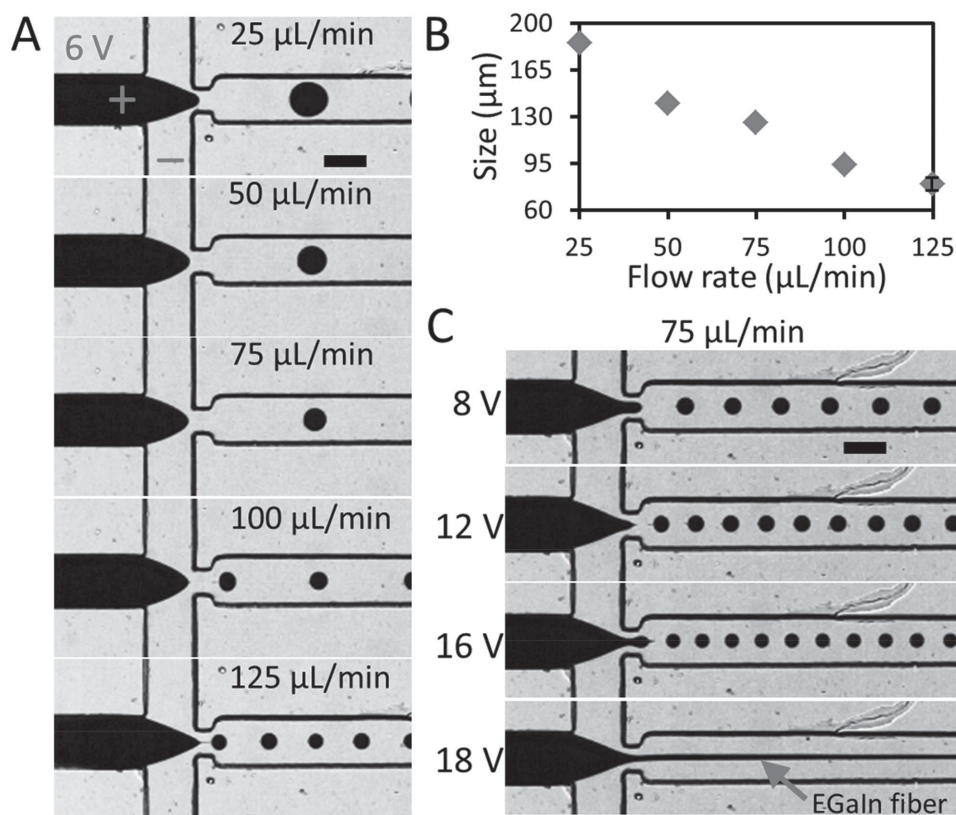


Figure 3. Investigating the smallest EGaIn microdroplet that can be produced using voltage in this system. A) Production of EGaIn microdroplets at different flow rates of the continuous phase liquid ranging from 25 to 125 $\mu\text{L min}^{-1}$. B) Droplet size versus glycerol–NaOH solution flow rate. C) Production of EGaIn microdroplets at voltages from 8 to 18 V, while setting the flow rates of glycerol–NaOH solution and EGaIn to 75 and 5 $\mu\text{L min}^{-1}$, respectively. Scale bars are 200 μm .

microdroplets. We sought to illustrate that this concept still holds even in the presence of potential and also produce the smallest droplets possible using the configuration depicted in Figure 1. **Figure 3A** shows the production of microdroplets at different flow rates of the glycerol–NaOH solution while maintaining the flow rate of EGaIn at 5 $\mu\text{L min}^{-1}$ and the voltage at 6 V. Under these conditions, the diameter of EGaIn microdroplets decreases from ≈ 186 to ≈ 80 μm by increasing the flow rate of the solution of glycerol–NaOH from 25 to 125 $\mu\text{L min}^{-1}$. **Figure 3B** shows that the change of microdroplet size is almost linear with respect to the flow rate of the continuous phase liquid. However, applying flow rates greater than 75 $\mu\text{L min}^{-1}$ generates sufficient pressure to deform the plastic syringe and tubing leading to the inlet. The deformation of the syringe compromises the stability of the flow-focusing system, and leads to the formation of nonuniform sized microdroplets, which is most obvious at a flow rate of 125 $\mu\text{L min}^{-1}$ (as apparent in the image in **Figure 3A** and quantified by the error bar in **Figure 3B**).

Setting the flow rate of the glycerol–NaOH solution to 75 $\mu\text{L min}^{-1}$ and increasing the magnitude of DC voltage from 8 to 16 V decreases the diameter of EGaIn microdroplets from ≈ 90 to 75 μm (**Figure 3C**), which is 25% smaller than W_{orifice} (**Movie S3**, Supporting Information). Interestingly, applying a DC voltage of 18 V causes the formation of an EGaIn fiber with a diameter of ≈ 30 μm along the microchannel (**Figure 3C**),

indicating the limitation of the device for producing smaller microdroplets. The EGaIn fiber becomes unstable downstream in the microchannel and breaks up into nonuniform sized microdroplets (**Movie S3**, Supporting Information).

Changing the flow rate of either continuous or discrete phase liquids is an effective means to tune the diameter of microdroplets with monodisperse sizes. However, it takes a relatively long time (15–30 s) to reach stable conditions after changing the flow rate and thus, the quality of droplets produced during periods of transition are unpredictable and uncontrolled. As such, we further examine the capability of this electrical method for instantaneous control over the size of EGaIn microdroplets by applying an AC signal.

Figure 4A shows the production of EGaIn droplets when applying a 1 Hz square wave with a magnitude of 5 V, while the flow rate of glycerol–NaOH and EGaIn are set to 75 and 5 $\mu\text{L min}^{-1}$, respectively (**Movie S4**, Supporting Information). These conditions produce uniform EGaIn microdroplets with two different diameters dictated by the applied voltage. More importantly the diameter of the microdroplets changes quickly in response to the AC square wave. Videos from a high speed camera suggest the transition time required for stabilizing the size of the produced microdroplets is only ≈ 30 ms after switching between positive and negative voltages. For the conditions in **Figure 4A**, only one droplet forms during this transition period. In addition, the size difference of the microdroplets can

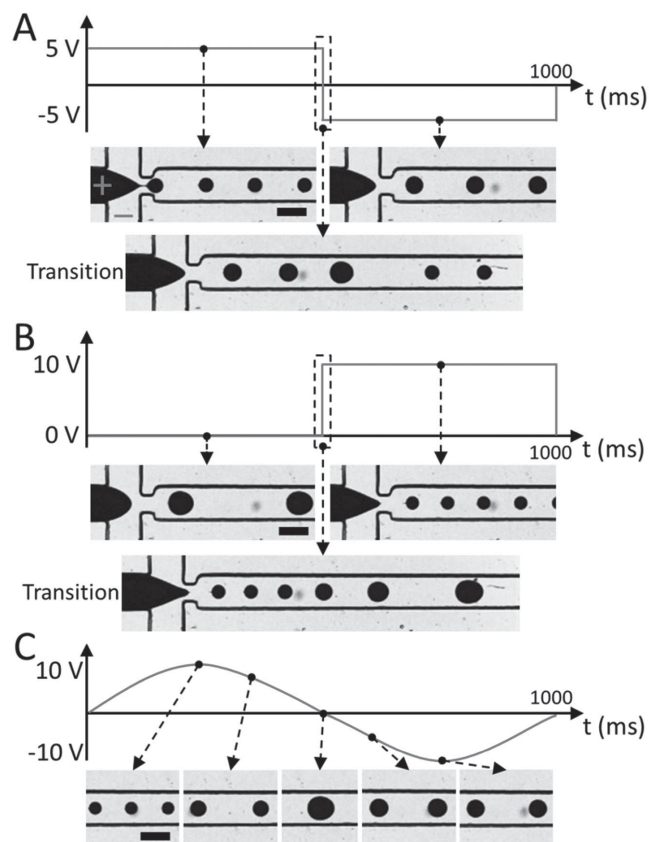


Figure 4. Dynamic control over the size of EGaIn microdroplets. Production of EGaIn microdroplets using A) square wave signal with 5 V magnitude and 0 V offset at a frequency of 1 Hz, B) square wave signal with 5 V magnitude and 5 V DC offset at a frequency of 1 Hz, and C) sinusoidal wave signal with 10 V magnitude and a frequency of 1 Hz. Scale bars are 200 μm .

be increased by adding a DC offset to the applied signal, as shown in Figure 4B (see Movie S5, Supporting Information, for the case when a 4 Hz signal is applied).

Changing the potential alters the surface tension and therefore the diameter and thus frequency of formation of the microdroplets. Droplet formation is complex, but to a first approximation, it is sensible to utilize AC frequencies less than or equal to the frequency of droplet formation so that: i) the droplets experience a single potential as they pass through the orifice; and ii) the potential does not change more than once between formation of sequential droplets. For these flow conditions, droplets form every ≈ 20 ms at 0 V and every ≈ 7 ms at 10 V. Thus, the frequency should not be greater than 50–142 Hz. Choosing a frequency also involves considerations of the time necessary to stabilize droplet formation. Since the time necessary to stabilize droplets (≈ 30 ms) is longer than the time necessary to form a single droplet (≈ 7 – 20 ms), at least one droplet will form during this transition period, and consequently will have an intermediate diameter as the system transitions through a change in voltage. Although not ideal, the transition period, shown in Figure 4A,B, affects the diameter in a reproducible way. Ultimately, the particle distribution represents a superposition of the AC signal and the frequency of droplet formation, while accounting for the role of the transition period

on droplet size. In our experiments, we found that two or more sequential droplets with the same size form only if the frequency of the signal is below 15 Hz, as shown in Supporting Information, Section S3.

This approach can produce various sizes of EGaIn microdroplets by applying a sinusoidal signal, in which the size of the produced microdroplets changes smoothly according to the magnitude of the voltage, as shown in Figure 4C. This enables a repeating train of microdroplets with varying sizes ranging from ≈ 85 to ≈ 185 μm along the channel, which is not achievable by varying the flow rate of either continuous or discrete phase liquids. Our method, therefore, enables the formation of narrowly defined, multimodal size distributions and frequencies (i.e., streams of droplets with more than one diameter) or broad distributions depending on the nature of the signal.

In summary, we demonstrate a novel method for controlling the size of liquid-metal microdroplets produced in a microfluidic flow-focusing system using only voltage to control the surface tension of the metal. The method can decrease the diameter of liquid-metal microdroplets by a factor of two, although it may be possible to go even smaller with larger voltages. Moreover, the diameter of the microdroplets can be $\approx 25\%$ smaller than the width of the orifice, whereas the smallest previously reported droplets were greater than or equal to the orifice. To utilize electrocapillarity to modulate interfacial tension, the continuous and discrete phases need to be conductive and immiscible. Here, we utilized liquid metal as the discrete phase, but it may be possible to use it as the continuous phase or replace it with other conductive fluids, such as ionic liquids. Most importantly, our method is able to control and change the size of sequential microdroplets simply by changing the magnitude of the voltage. The droplet diameter responds significantly faster than changes achieved by varying the flow rate of either continuous or discrete phase liquids. As a consequence, it is possible to instantaneously tune the diameter and thus, frequency of droplets such that a single stream can contain droplets with a controlled distribution of diameters. This ability may be useful for collecting narrowly defined, multimodal distributions of particles for improved colloidal packing, microfluidic logic or optical devices,^[22,23,33] colloidal inks,^[19] or composites that utilize liquid metals.^[18] Thus, this method has the potential to enable practical applications of droplet-based liquid-metal systems in the areas of microfluidics, optics and microelectromechanical systems (MEMS).

Experimental Section

Materials: EGaIn was purchased from Indium Corporation, USA. Glycerol and solid NaOH were purchased from Sigma Aldrich, USA. The PDMS microchannel was fabricated using standard soft lithography techniques,^[34] and subsequently bonded onto a glass slide after oxygen plasma treatment.

Experimental Setup: Two syringe pumps (Fusion 100, Chemyx) injected glycerol–NaOH solution and EGaIn liquid metal into the microfluidic chip. The formation of liquid metal microdroplets was monitored using a high-speed camera (Phantom v4.2, Vision Research Inc.) fitted onto an inverted microscope (Olympus, GX71). A DC signal generator (HY1803D, Tekpower) and an AC signal generator (Model 645, Duncan Instruments) applied desired voltages to control the interfacial tension of the liquid metal, and the current was measured using a multimeter (34401A, Agilent).

Liquid-Metal Interfacial Tension Measurement: The interfacial tension between EGaIn and glycerol–NaOH solution was measured by a goniometer (First Ten Angstroms 1000B), with a potentiostat (Reference 600, Gamry Instrument) used for providing current.

Supporting Information

Supporting Information is available from the Wiley Online Library or from the author.

Acknowledgements

M.D.D. acknowledges support from the Air Force Research Laboratory, the NSF CAREER Award (CAREER CMMI-0954321), and the Research Triangle NSF MRSEC on Programmable Soft Matter (DMR-1121107).

Received: August 9, 2015

Revised: October 9, 2015

Published online: November 25, 2015

-
- [1] M. D. Dickey, *ACS Appl. Mater. Interfaces* **2014**, *6*, 18369.
- [2] T. Liu, P. Sen, C.-J. Kim, *J. Microelectromech. Syst.* **2012**, *21*, 443.
- [3] J. H. So, J. Thelen, A. Qusba, G. J. Hayes, G. Lazzi, M. D. Dickey, *Adv. Funct. Mater.* **2009**, *19*, 3632.
- [4] H. J. Koo, J. H. So, M. D. Dickey, O. D. Velev, *Adv. Mater.* **2011**, *23*, 3559.
- [5] E. Palleau, S. Reece, S. C. Desai, M. E. Smith, M. D. Dickey, *Adv. Mater.* **2013**, *25*, 1589.
- [6] D. Kim, R. G. Pierce, R. Henderson, S. J. Doo, K. Yoo, J. B. Lee, *Appl. Phys. Lett.* **2014**, *105*, 234104.
- [7] J. Yoon, S. Y. Hong, Y. Lim, S. J. Lee, G. Zi, J. S. Ha, *Adv. Mater.* **2014**, *26*, 6580.
- [8] Y. L. Park, C. Majidi, R. Kramer, P. Bérard, R. J. Wood, *J. Microeng. Microeng.* **2010**, *20*, 125029.
- [9] Y. L. Park, D. Tepayotl-Ramirez, R. J. Wood, C. Majidi, *Appl. Phys. Lett.* **2012**, *101*, 191904.
- [10] S.-Y. Tang, V. Sivan, P. Petersen, W. Zhang, P. D. Morrison, K. Kalantar-Zadeh, A. Mitchell, K. Khoshmanesh, *Adv. Funct. Mater.* **2014**, *24*, 5851.
- [11] S.-Y. Tang, K. Khoshmanesh, V. Sivan, P. Petersen, A. P. O'Mullane, D. Abbott, A. Mitchell, K. Kalantar-Zadeh, *Pro. Natl. Acad. Sci. USA* **2014**, *111*, 3304.
- [12] W. Zhang, J. Z. Ou, S. Y. Tang, V. Sivan, D. D. Yao, K. Latham, K. Khoshmanesh, A. Mitchell, A. P. O'Mullane, K. Kalantar-Zadeh, *Adv. Funct. Mater.* **2014**, *24*, 3799.
- [13] V. Sivan, S. Y. Tang, A. P. O'Mullane, P. Petersen, N. Eshtiaghi, K. Kalantar-Zadeh, A. Mitchell, *Adv. Funct. Mater.* **2013**, *23*, 144.
- [14] P. Sen, C.-J. Kim, *IEEE Trans. Ind. Electron.* **2009**, *56*, 1314.
- [15] J. Zhang, Y. Yao, L. Sheng, J. Liu, *Adv. Mater.* **2015**, *26*, 2648.
- [16] S.-Y. Tang, J. Zhu, V. Sivan, B. Gol, R. Soffe, W. Zhang, A. Mitchell, K. Khoshmanesh, *Adv. Funct. Mater.* **2015**, *25*, 4445.
- [17] C. Ladd, J. H. So, J. Muth, M. D. Dickey, *Adv. Mater.* **2013**, *25*, 5081.
- [18] A. Fassler, C. Majidi, *Adv. Mater.* **2015**, *27*, 1928.
- [19] J. W. Boley, E. L. White, R. K. Kramer, *Adv. Mater.* **2015**, *27*, 2355.
- [20] T. Krupenkin, J. A. Taylor, *Nat. Commun.* **2011**, *2*, 448.
- [21] L. Zou, W. Withayachumnankul, C. M. Shah, A. Mitchell, M. Bhaskaran, S. Sriram, C. Fumeaux, *Opt. Express* **2013**, *21*, 1344.
- [22] M. Hashimoto, B. Mayers, P. Garstecki, G. M. Whitesides, *Small* **2006**, *2*, 1292.
- [23] J. Yu, Y. Yang, A. Liu, L. Chin, X. Zhang, *Opt. Lett.* **2010**, *35*, 1890.
- [24] J. N. Hohman, M. Kim, G. A. Wadsworth, H. R. Bednar, J. Jiang, M. A. LeThai, P. S. Weiss, *Nano Lett.* **2011**, *11*, 5104.
- [25] M. G. Mohammed, A. Xenakis, M. D. Dickey, *Metals* **2014**, *4*, 465.
- [26] J. Thelen, M. D. Dickey, T. Ward, *Lab Chip* **2012**, *12*, 3961.
- [27] B. Gol, F. J. Tovar-Lopez, M. E. Kurdzinski, S.-Y. Tang, P. Petersen, A. Mitchell, K. Khoshmanesh, *Lab Chip* **2015**, *15*, 2476.
- [28] T. Hutter, W. A. C. Bauer, S. R. Elliott, W. T. Huck, *Adv. Funct. Mater.* **2012**, *22*, 2624.
- [29] S.-Y. Teh, R. Lin, L.-H. Hung, A. P. Lee, *Lab Chip* **2008**, *8*, 198.
- [30] W. Lee, L. M. Walker, S. L. Anna, *Phys. Fluids* **2009**, *21*, 032103.
- [31] M. R. Khan, C. B. Eaker, E. F. Bowden, M. D. Dickey, *Proc. Natl. Acad. Sci. USA* **2014**, *111*, 14047.
- [32] D. C. Grahame, *Chem. Rev.* **1947**, *41*, 441.
- [33] M. Prakash, N. Gershenfeld, *Science* **2007**, *315*, 832.
- [34] K. Kalantar-Zadeh, B. Fry, *Nanotechnology-Enabled Sensors*, Springer Science & Business Media, New York **2007**.
-